Journal Pre-proof

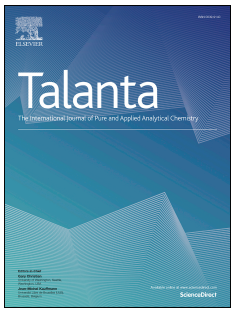

Fabrication of Au nanoclusters confined on hydroxy double salt-based intelligent biosensor for on-site monitoring of urease and its inhibitors

Yaqing Han, Mengke Wang, Han Xie, Yitong Zhou, Shun Wang, Guannan Wang

PII: S0039-9140(24)00104-8

DOI: https://doi.org/10.1016/j.talanta.2024.125725

Reference: TAL 125725

To appear in: *Talanta*

Received Date: 30 November 2023

Revised Date: 16 January 2024

Accepted Date: 26 January 2024

Please cite this article as: Y. Han, M. Wang, H. Xie, Y. Zhou, S. Wang, G. Wang, Fabrication of Au nanoclusters confined on hydroxy double salt-based intelligent biosensor for on-site monitoring of urease and its inhibitors, *Talanta* (2024), doi: https://doi.org/10.1016/j.talanta.2024.125725.

Graphical Abstract

In this work, the gold nanoclusters (AuNCs) and hydroxyl double salt (HDS) were composited by a simple confinement effect to prepare highly fluorescent AuNCs@HDS composites. Based on the sensitive response of AuNCs@HDS to pH, a highly efficient sensing platform for pH-related enzyme urease and its drug inhibitors detection was constructed for the first time.

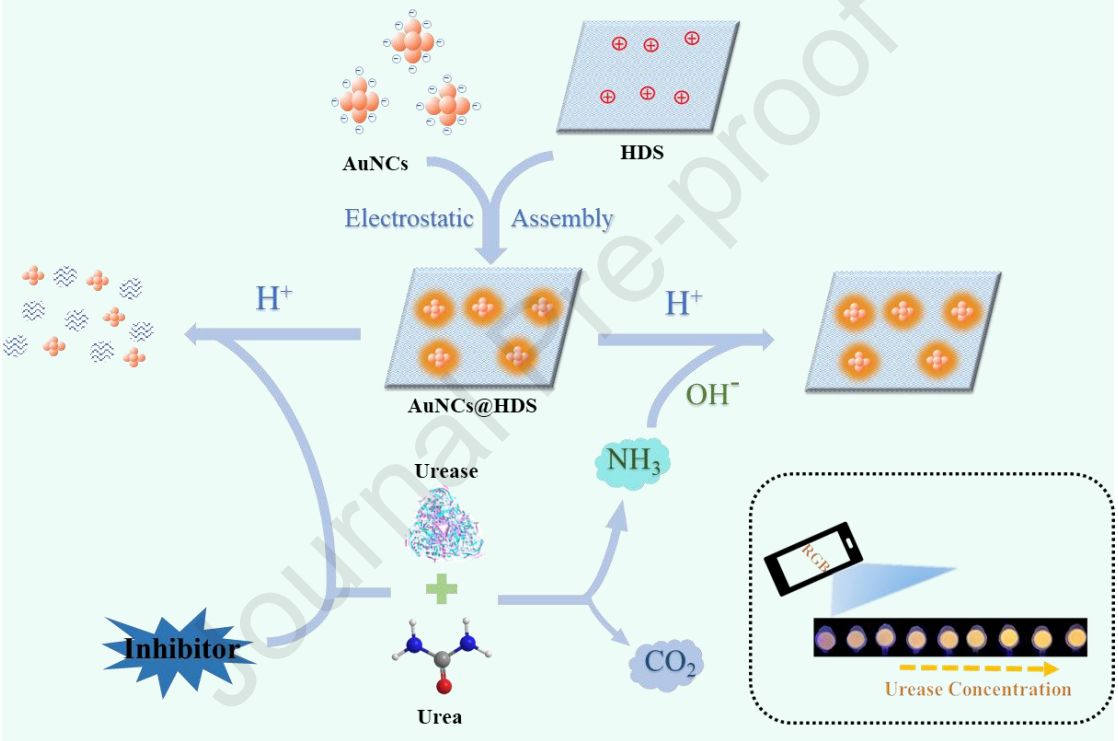

Fabrication of Au nanoclusters confined on hydroxy double salt-based intelligent biosensor for on-site monitoring of urease and its inhibitors

Yaqing Han [a,b], Mengke Wang [b], Han Xie [c], Yitong Zhou [c], Shun Wang [b]*, and Guannan Wang[c,b]*

[a] Shandong First Medical University & Shandong Academy of Medical Sciences, Jinan, 250117, P. R. China

[b] College of Medical Engineering & the Key Laboratory for Medical Functional Nanomaterials, Jining Medical University, Jining 272067, P. R. China

[c] Shenyang Key Laboratory of Medical Molecular Theranostic Probes, School of Pharmacy, Shenyang Medical University, Shenyang, 110034, P. R. China

*Corresponding author

E-mail address: wshun155@163.com (Dr. Shun Wang)

chemwangguannan@gmail.com (Pro. Guannan Wang)

Abstract

Sensitive and convenient sensing of urease and its inhibitors is exceptionally urgent in clinical diagnosis and new drug development. In this study, the gold nanoclusters (AuNCs) and hydroxyl double salt (HDS) were composited by a simple confinement effect to prepare highly fluorescent AuNCs@HDS composites to monitor urease and its drug inhibitors. HDS was used as a matrix to confine AuNCs (AuNCs@HDS), facilitating the emission intensity of AuNCs. However, acidic conditions (low pH) can disrupt the structure of HDS to break the confinement effect, and quench the fluorescence of AuNCs. Therefore, a sensing platform for pH-related enzyme urease detection was constructed based on the sensitive response of AuNCs@HDS to pH. This sensing platform had a linear response range of 0.5-22.5 U/L and a low limit of detection (LOD) of 0.19 U/L for urease. Moreover, this sensing platform was also applied to monitor urease inhibitors and urease in human saliva samples. Additionally, a portable hydrogel kit combined with a smartphone was developed for urease detection to achieve portable, low-cost, instrument-free, and on-site monitoring of urease.

Keywords: Fluorescent sensing; Gold nanoclusters; Confinement effect; Urease activity; Hydrogel kit

1. Introduction

Urease was the first prepared crystalline enzyme [1]. It was also the first discovered nickel-containing metal enzyme [2] and is ubiquitous in bacteria, fungi, animals, and plants [3]. Although urease from different sources varies in subunits, they have highly conserved tertiary structures and similar catalytic functions [4]. Urease catalyzes the hydrolysis of urea to carbon dioxide and ammonia [5]. The overexpression of bacterial urease in the human body can damage the cells of living systems [6, 7], and is, therefore, closely related to the onset of clinical symptoms caused by bacterial infections. These include urinary stones, pyelonephritis, hepatic coma, and peptic ulceration [8, 9]. Urease inhibition is a crucial method for treating diseases caused by urease-producing bacteria [10, 11]. Thus, it is crucial to advance biomedicine to create practical and affordable methods for the sensitive and precise detection of urease activity and its inhibitors.

So far, various analytical techniques have been applied in urease detection, such as fluorimetry [12-14], electrochemistry [15] and colorimetry [16]. Among them, the fluorescence method is widely used owing to its fast response and high sensitivity. Consequently, many fluorescent sensors based on various nanomaterials have been developed for urease detection, such as carbon dots [17], graphene quantum dots [18], silica dots [19], and gold nanoclusters [20]. Shi et al. described a turn-on fluorescent test that used chitosan and reduced graphene quantum dots as an integrative self-assembly probe to selectively and sensitively assess urease activity [18]. By the N-acetylcysteine-directed synthesis of fluorescent AuNCs, Deng's group created a practical fluorescent sensor for measuring urease activity and inhibitor [20]. However, these urease detection procedures often require complex experimental operations or the synthesis of special materials. Therefore, it is the need of the hour to develop a convenient and efficient method for measuring urease and inhibitors.

Gold nanoclusters (AuNCs) have attracted the attention of the biomedical research community due to their excellent optical stability and biocompatibility [21-23]. Among the many methods for synthesizing AuNCs, the template method is the most commonly

used for preparing gold nanoclusters [24, 25]. Accordingly, AuNCs with varied optical properties can be prepared using different templates [26, 27]. Although AuNCs have excellent physical and chemical properties, their relatively low quantum yield (QY) limits their biosensing applications. Various methods have been proposed to compound fluorescent AuNCs with other matrix materials to prepare highly fluorescent AuNCs-based composite probes to address the problem of low QY of AuNCs [28, 29]. Among them, the noncovalent interaction-based way is a convenient strategy. In order to immobilize weak fluorescent AuNCs on the SiO_2 surface, Cai's group used electrostatic adsorption [30]. This excited the aggregation-induced emission (AIE) features of the AuNCs, which in turn amplified the fluorescent signal. Thus, a current research hotspot is a simple method to synthesize AuNCs-based composite fluorescent probes with excellent fluorescence performance.

Layered double hydroxide (LDH) is a two-dimensional (2D) layered material consisting of positively charged layers with charge-balancing anions and water molecules between the layers [31]. Due to its low toxicity and good biocompatibility, LDH is crucial as host matrices in catalysis, biology, optical devices, and electrochemical sensors [32, 33]. Hydroxyl double salt (HDS), a related family of LDH, has a much higher charge density [34], suitable for enhancing the fluorescence of AuNCs [31]. Considering these properties, HDS was used as a host material to prepare AuNCs@HDS by electrostatic interaction for biosensing.

Inspired by the studies discussed above and previous work done by this research group [35], a simple electrostatic interaction strategy was utilized to confine glutathione stabilized AuNCs onto the surface of zinc-containing HDS (AuNCs@HDS) to substantially enhance the AuNCs fluorescence, which exhibits typically fluorescent response to acid (H^+). Based on this fact, a simple and efficient fluorescence detection platform was constructed for urease and its inhibitors using AuNCs@HDS as a probe (**Scheme 1**). After adding H^+, the HDS was hydrolyzed, and subsequently, the surface confinement effect of HDS was disrupted, resulting in the fluorescence quenching of AuNCs@HDS. When urea and urease were introduced into the system, urease

hydrolyzed urea to produce OH^-, reducing H^+ in the system. Consequently, the fluorescence of AuNCs@HDS was restored. Urease inhibitors can inhibit the hydrolysis of urea by urease, and the fluorescence of AuNCs@HDS was quenched, thereby detecting urease inhibitors. This sensing platform was used to monitor urease activity in human saliva samples; the results were satisfactory. A portable hydrogel kit with agarose as the carrier was also developed to realize the visualization and quantitative on-site monitoring of urease.

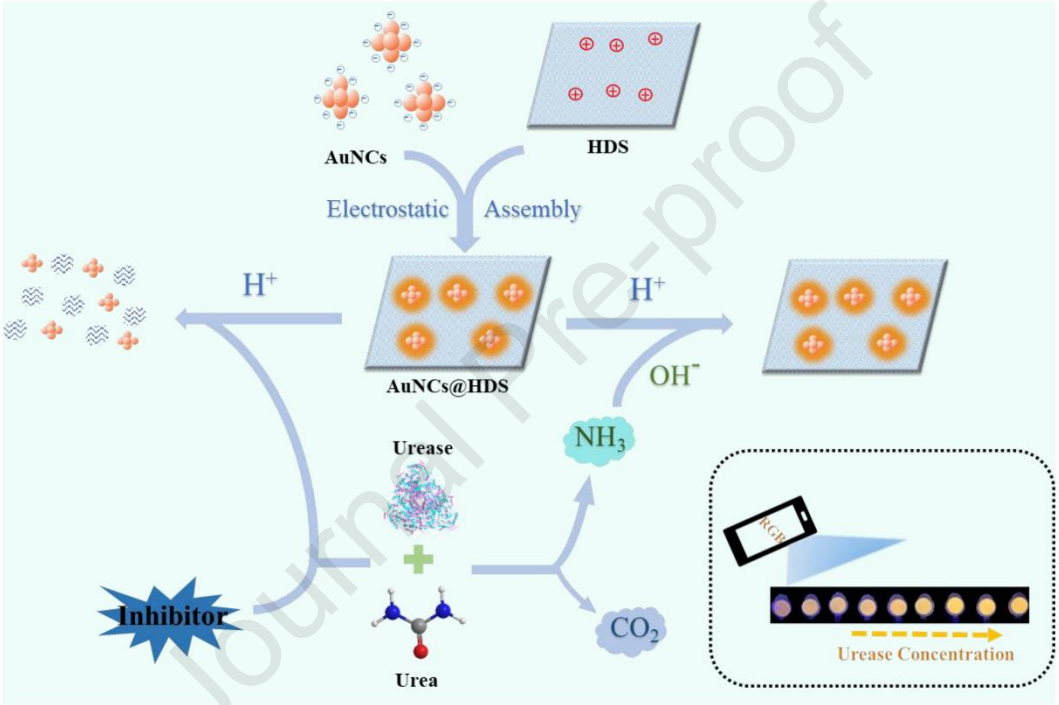

Scheme 1. Principle of the AuNCs@HDS fluorescence method for urease and urease inhibitor activity detection.

2. Experimental section

2. 1 Fabrication of AuNCs and AuNCs@HDS composite

For AuNCs, according to a previous report [36], 2 mL $HAuCl_4$ (10 mM) was added to 7.7 mL H_2O at 25 °C. GSH (300 μL,100 mM) was added dropwise under gentle stirring (500 rpm), and after the mixture was reacted for 5 minutes, heated to 70 °C for 24 h. Finally, the AuNCs solution was purified by a dialysis process (through a dialysis

bag with MWCO 1000 Da) for 24 h.

The AuNCs@HDS was prepared based on our previous work [35]. Briefly, AuNCs (500 μL, 1.5 mg/mL) and HDS (100 μL, 1.6 mg/mL) were added to 2.4 mL ultrapure water. The combined solution was permitted to react at room temperature for 2 hours. The supernatant was removed after centrifugation (rpm 10000, 15 min), and the precipitate was rehydrated to 3 mL. The AuNCs@HDS were obtained by ultrasonic dispersion.

2. 2 Fluorescence detection of urease activity

For urease detection, different concentrations of urease and urea solution (140 μL, 10 mM) were mixed with Tris-HCl buffer solution (pH=7.0, 10 μL, 10 mM), and the resulting mixture was incubated at 37 °C for 50 minutes. After that, the catalytic process was stopped by adding AuNCs@HDS (500 μL, 0.3 mg/mL) and acetic acid buffer solution (pH=3.5, 60 μL, 10 mM). After 3 minutes, the fluorescence spectra were recorded with an excitation wavelength of 405 nm.

2. 3 Urease inhibitor detection

To detect urease inhibitors, urease (30 μL, 1.0 U/mL) was reacted with different concentrations of urease inhibitors (AHA or dimethoate) at 37 ° C for 1 hour. Subsequently, urea (140 μL, 10 mM) and Tris-HCl buffer solution (pH=7.0, 10 μL, 10 mM) were introduced to the aforementioned solution, and the reaction was maintained at 37 °C for 50 minutes. The steps that followed were identical as those for the analysis of urease activity. The inhibition efficiency (IE, %) can be calculated by the following equation.

$$IE\ (\%) = (F' - F) / (F' - F_0) \times 100$$

In this formula, F_0 is the fluorescence intensity of AuNCs@HDS containing urea, F' is the fluorescence intensity of AuNCs@HDS containing urea and urease, and F is the fluorescence intensity of AuNCs@HDS containing urea, urease and inhibitor (AHA or dimethoate).

2. 4 Fabrication and application of a portable kit for urease

The agarose (4 mg) was mixed with ultrapure water (4 mL) and the mixture was heated at 100 °C until dissolved. When the aforementioned mixture was cooled to 50 °C, AuNCs@HDS (400 μL, 0.3 mg/mL) was added to it. After mixing well, 400 μL of the above solution was added to the centrifuge tube cap and cooled to obtain the AuNCs@HDS hydrogel. This hydrogel was stored at room temperature for further use.

To apply the prepared hydrogel for urease analysis, the reaction procedure in Section 2.2 was first carried out. After the end of the reaction, the reacted solution was allowed to react with the prepared hydrogel for 10 min by inverting the centrifuge tube. To identify urease quantitatively, the color of the hydrogel was captured under UV light using a smartphone (iPhone 14) and analyzed with the Color-Collection APP.

2. 5 Detection of urease in the saliva samples

Saliva samples were provided by informed volunteers. The assay for urease in saliva was performed as follows: first, the saliva samples were diluted 10-time and centrifuged to remove particulate matter from the saliva samples. After that, the pH of the saliva samples was brought to a neutral pH level of 7.0 by using HCl or NaOH on a PHS-3C pH meter. Finally, urease activity in the saliva samples was measured by means of the standard addition method.

3. Results and Discussion

3. 1 Characterization of AuNCs, HDS and AuNCs@HDS

The successful synthesis of AuNCs@HDS fluorescent composites was confirmed via TEM, SEM, and STEM. The morphology and particle size of AuNCs obtained by TEM (**Fig. 1A**) revealed that AuNCs were approximately spherical and well dispersed with an average particle size of ~2.04 nm (**Fig. 1A inset**). The SEM image of HDS in **Fig. 1B** showed the quadrilateral sheet of HDS with a size < 5 μm. The SEM image of AuNCs@HDS in **Fig. 1C** confirmed that after anchoring AuNCs, the surface of HDS exhibited a rough morphology. **Fig. 1D and Fig. 1E** showed the TEM images of AuNCs@HDS, and the uniformly dispersed AuNCs were observed in the HDS matrix.

Additionally, STEM was used to demonstrate the distribution of AuNCs on HDS. Also, **Fig. 1F and Fig. 1G** demonstrated the elemental mapping of Zn, Au, N, and S of AuNCs@HDS using EDS. These distribution ranges were aligned with the TEM images and the STEM image of AuNCs@HDS, indicating that the AuNCs were uniformly distributed on the HDS surface.

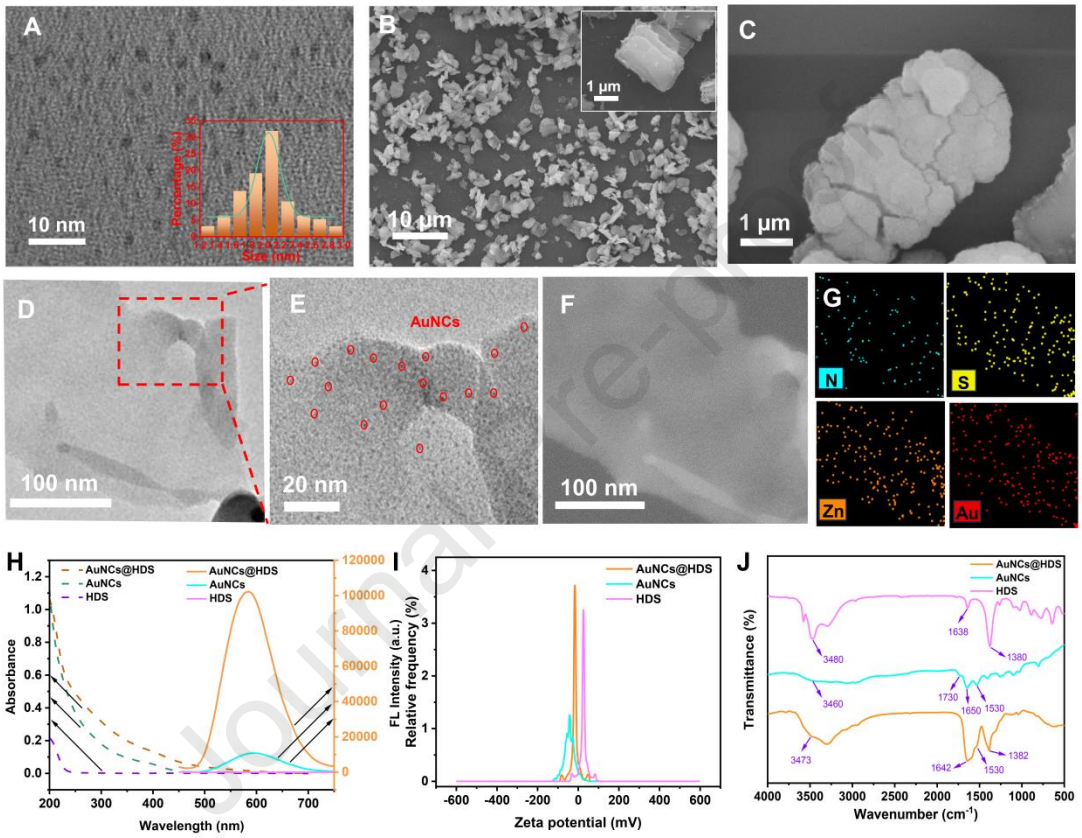

Fig. 1. (A) TEM pictures of AuNCs. (B, C) SEM pictures of HDS. (D, E) TEM images of AuNCs@HDS. (F) STEM images and the Zn, Au, N, and S elemental mapping images (G) of AuNCs@HDS. (H) Ultraviolet-visible absorption spectra and fluorescence spectra, (I) Zeta potentials, and (J) FT-IR spectra of AuNCs@HDS, AuNCs and HDS, separately.

The successful synthesis of AuNCs@HDS was further confirmed by UV-Vis absorption spectra, fluorescence spectra, zeta potentials, XRD patterns, and FT-IR spectra. A previous study from our group have systematically demonstrated that the HDS could efficiently enhance the fluorescence of AuNCs simply through the surface

confinement effect [35]. Briefly, when the excited electrons and holes are effectively confined by the HDS with a broad band gap, it can promote the radiation transition and enhanced fluorescence performances of AuNCs. As revealed in **Fig. 1H,** compared with AuNCs, the fluorescence intensity of AuNCs@HDS strengthened 8-fold. This UV-Vis absorption spectra showed that the entire absorption spectra of AuNCs showed only a slight upshift after AuNCs were confined to the HDS surface. According to the zeta potentials (**Fig. 1I** and **Fig. S2**), HDS had a positively charged state with an average zeta potential of +24.97 mV, AuNCs had a negatively charged state with an average zeta potential of −48.56 mV, and the combination of AuNCs and HDS displayed a partially neutralized zeta potential of −16.63 mV. Therefore, AuNCs were adsorbed and confined to the surface of HDS via electrostatic interactions, forming AuNCs@HDS.

The FT-IR spectra of AuNCs@HDS, AuNCs and HDS are shown in **Fig. 1J.** The O-H stretching vibrations that produced the peaks at 3480 cm^{-1} and 1638 cm^{-1} suggest that HDS contains hydroxyl groups. The N-O stretching vibrations at 1380 cm^{-1} confirmed the nitrate anion in HDS [31]. For AuNCs, the vibrations at 1730 cm^{-1} (C=O stretching), at 3460 $cm^{-1,}$ and 1650 cm^{-1} (O-H stretching) indicated the presence of carboxyl groups on the surface of AuNCs [37, 38]. Additionally, characteristic stretching vibrations of N-H was shown at 1530 cm^{-1} [38]. The successful complexation of AuNCs on the surface of HDS was demonstrated by similar absorption peaks from HDS and AuNCs in the AuNCs@HDS spectrum.

The XRD patterns of AuNCs@HDS, AuNCs and HDS are displayed in **Fig. S3**. The typical diffraction peaks of HDS correspond to the (003), (006), and (009) diffraction peaks of HDS, indicating that HDS possessed a highly crystalline phase [31, 39]. A characteristic (111) diffraction peak at 33° was observed in the XRD spectrum of AuNCs [40]. The distinctive diffraction peaks of HDS and AuNCs were seen in the XRD pattern of AuNCs@HDS, confirming the effective synthesis of AuNCs@HDS.

3. 2 pH sensing mechanism and feasibility analysis of urease

AuNCs@HDS was used as the probe to establish a highly selective and sensitive urease detection platform. **Scheme 1** shows the mechanism of urease detection. First,

AuNCs were adsorbed and confined to the surface of HDS via electrostatic interactions, enhancing the fluorescence of AuNCs. Next, based on the previous synthetic research [31], as HDS is a related family of LDHs with formula $[Zn_5(OH)_8]$ $(NO_3)_2 \cdot nH_2O$, H^+ can combine with OH^- in the structure, thereby disrupting its layered structure to destroy its surface confinement effect and lead to a significant quenching of the fluorescence of AuNCs. Also, urease specifically hydrolyzed urea to generate ammonia, thus, urease activity increased the concentration of OH^- in the solution, which consumed H^+ and restored the fluorescence of AuNCs@HDS. Urease could be detected based on the changes in fluorescence intensity in the system. Thus, the following experiments were conducted further to validate the principle and feasibility of this scheme.

The fluorescence intensity of AuNCs@HDS exhibited a quick quenching tendency in 3 minutes (**Fig. S4)**. The fluorescence at 585 nm of AuNCs@HDS showed a quenching tendency as the pH changed from 10.0 to 3.0 (**Fig. 2A)**. However, the fluorescence intensity of AuNCs did not change significantly with change in pH (**Fig. 2B**). At pH 3.0, the fluorescence intensity of AuNCs@HDS decreased to an intensity similar to that generated by AuNCs alone. The orange fluorescence of AuNCs@HDS gradually dimmed as the pH changed from 10.0 to 3.0 under UV light, while the fluorescence of individual AuNCs remained almost unchanged (**Fig. 2A** and **Fig. 2B inset)**. **Fig. 2C** showed that the fluorescence intensity of AuNCs@HDS depended on the pH. Furthermore, the fluorescence intensity of AuNCs@HDS was linearly correlated with the H^+ concentration, indicating that the AuNCs@HDS-based probe could be used for pH-related sensing applications (**Fig. S5)**.

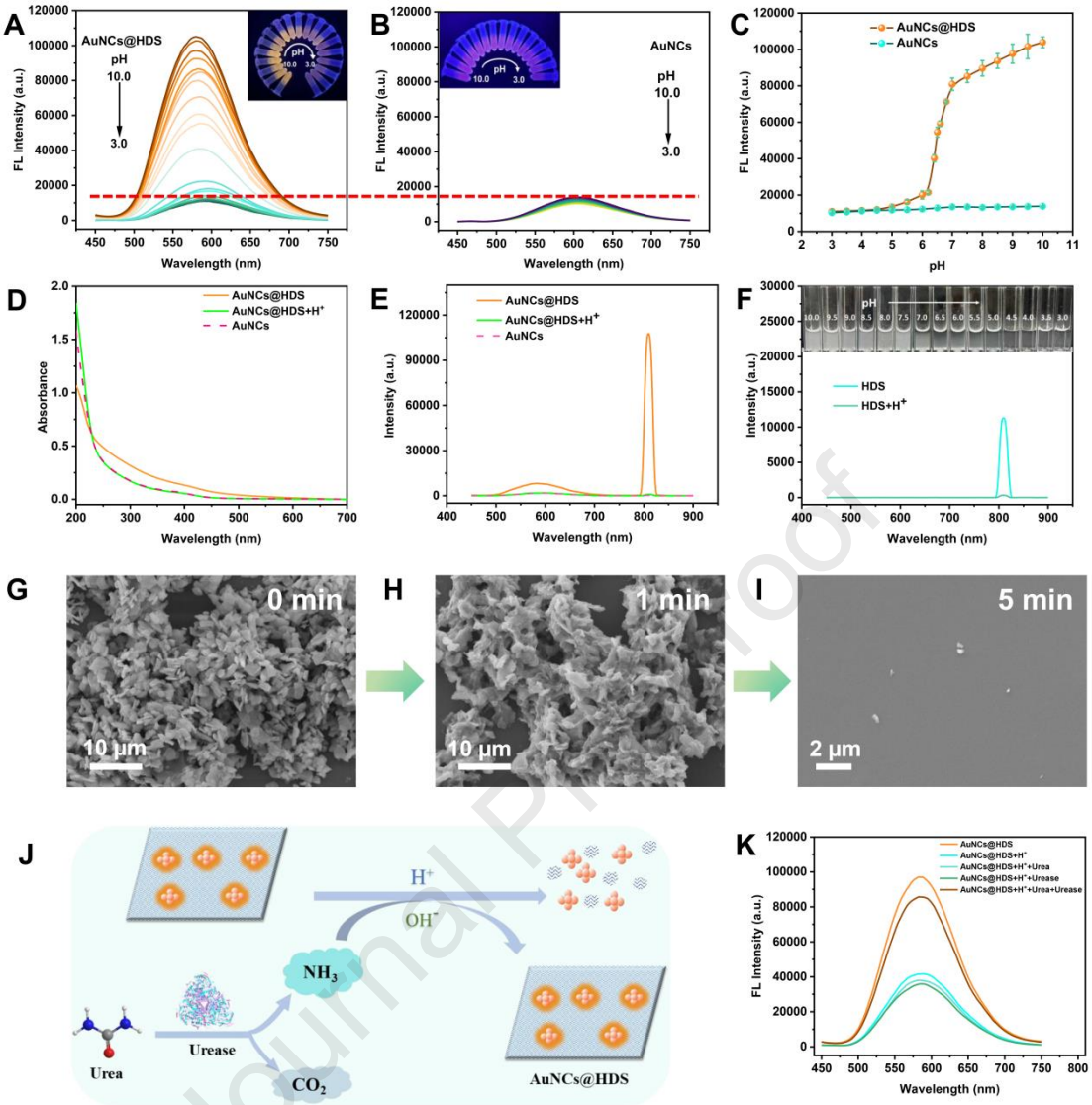

Fig. 2. (A, B) The fluorescence spectra of AuNCs@HDS and AuNCs with various pH concentrations. Inset: the corresponding fluorescence pictures under ultraviolet light (365 nm). (C) Relationship between fluorescence intensity (AuNCs@HDS and AuNCs) and different pH. (D, E) UV–Vis absorption spectra and secondary scattering spectra of AuNCs, AuNCs@HDS, and AuNCs@HDS + H^+. (F) The secondary scattering spectra of HDS and HDS + H^+. Figure inset: the corresponding images of HDS with different pH. (G-I) The SEM images of HDS were collected at different times after adding H^+. (J) Diagram depicting the fluorescence sensing platform for urease activity detection based on AuNCs@HDS. (K) FL spectra of the AuNCs@HDS system with blank, H^+, urea, urease, and urea/urease.

Next, the H^+-induced quenching mechanism of AuNCs@HDS was investigated

using UV-visible absorption spectroscopy, secondary scattering (SOS) spectroscopy, and SEM characterizations. The UV-visible absorption spectra showed that the absorption spectra of AuNCs@HDS were consistent with that of pure AuNCs after the addition of H^+, indicating that H^+ modified the structure of HDS to release AuNCs (**Fig. 2D)**. **Fig. 2E** exhibits the SOS patterns of AuNCs and AuNCs@HDS before and after addition of H^+. It could be seen that the SOS intensity of AuNCs@HDS was strongest before the addition of H^+, indicating that the particle size of AuNCs@HDS was the highest. After adding H^+, the SOS intensity of AuNCs@HDS was significantly reduced and was similar to that of AuNCs, indicating that the addition of H^+ destroyed the composite structure of AuNCs@HDS. **Fig. 2F** shows that adding H^+ significantly decreased the SOS intensity of HDS, indicating that H^+ destroyed the structure of HDS. **Fig. 2F inset** also shows that the HDS solution gradually became transparent from white turbidity as the pH decreased from 10.0 to 3.0. Also, **Fig. 2G-I** show SEM images of HDS at different times after adding H^+. Thus, HDS was in a relatively regular shape initially (**Fig. 2G**), which changed rapidly to an irregular state after the addition of H^+ (1 min) (**Fig. 2H**); the SEM image showed that the HDS was almost completely hydrolyzed after 5 min (**Fig. 2I**). These results indicated that H^+ could efficiently hydrolyze HDS, which caused fluorescence quenching of AuNCs@HDS.

Since the AuNCs@HDS system had good sensitivity and fast response to acidity and alkalinity (pH), the AuNCs@HDS probe was used for monitoring bio-enzyme associated with physiological pH changes (**Fig. 2J**). **Fig. S6** illustrates that urea urease and urea/urease did not affect the fluorescence of AuNCs or AuNCs@HDS. The fluorescence of AuNCs@HDS was dramatically quenched by H^+, as seen in **Fig. 2K.** Adding individual urea or urease had no recovery impact on the fluorescence of the AuNCs@HDS/H^+ system. However, the fluorescence of AuNCs@HDS was restored after adding urease/urea to the AuNCs@HDS system. These results indicated that this assay was feasible for urease activity detection.

3. 3 Detection of urease activity

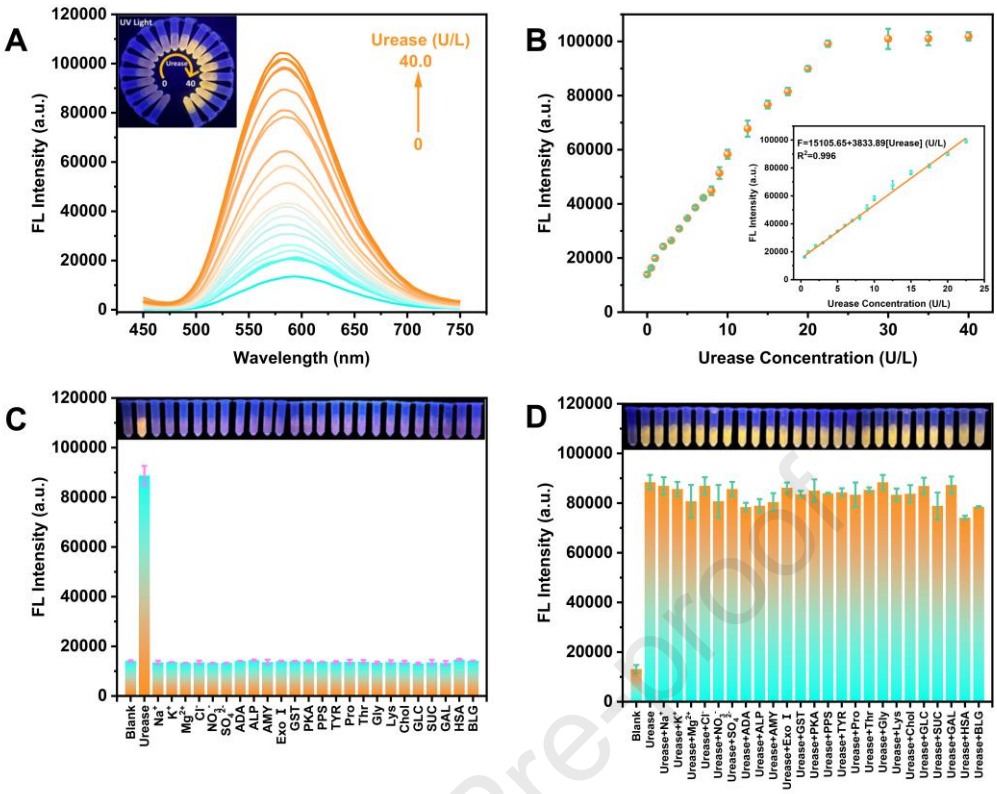

Fig. 3. (A) Fluorescence spectra and (B) intensity of AuNCs@HDS/H^+/urea system with different urease. Inset (A): the matching fluorescent pictures under UV (365 nm) light. Selectivity (C) and anti-interference ability (D) of the AuNCs@HDS-based method for urease detection. Concentrations: 22.5 U/L urease, 90.0 U/L other biological enzyme, 25 mg/L protein, 100 μM amino acids, 50 μM ions, and other bio-molecules.

The analytical performance of this fluorescent method was investigated to determine urease concentration under the established best experimental conditions (**Fig. S7**). **Fig. 3A** shows the fluorescence spectra of the AuNCs@HDS/H^+/urea system at different urease concentrations. With an increase in urease concentration, the fluorescence intensity of the AuNCs@HDS/H^+/urea system gradually increased, and the fluorescent color of the solution gradually brightened (**Fig. 3A, Fig. 3A** inset). In the range of 0.5 to 22.5 U/L, it was a strong linear relationship between the fluorescence intensity of the system and urease amount (**Fig. 3B**). The linear regression equation was: F = 15105.65 + 3833.89 [urease] (U/L), with a linear correlation coefficient (R^2) of 0.998, and a LOD value of 0.19 U/L. Also, this method was contrasted with previously

published urease analysis approaches. (**Table S1**). The outcomes demonstrated that the established fluorescence methods for detecting urease had a wide detection range and low detection limit, suggesting the urease detection method was capable and sensitive.

The selectivity and anti-interference ability of the urease detection platform offer several advantages for practical applications. Herein, common biological substances, including ions, biological enzymes, amino acids, proteins and other biomolecules, to simulate the complex biological matrices were selected to assess the distinctiveness of the urease detection based on the AuNCs@HDS sensor platform. The fluorescence intensity significantly increased when urease was introduced to the AuNCs@HDS/H^+/urea detection system (**Fig. 3C**), while it remained unchanged in the presence of other substances, indicating that this assay was highly selective for urease sensing. Furthermore, the interference experiment showed that when the urease in the detection system coexisted with other interfering substances, the fluorescence of the system remained unaffected, indicating that the urease assay had good anti-interference ability (**Fig. 3D**). These findings suggested that this sensing platform had reasonable specificity for detecting urease activity in biological samples.

The factors that contribute to the high precision and repeatability of urease measurement systems can be summarized as follows: (1) The recognition of urease to its catalytic substrate ensure the specificity. (2) Fluorescence methods have many advantages of high sensitivity and efficiency. Besides, HDS, as a carrier, can enhance the fluorescence of AuNCs while also being sensitive to H^+, significantly improving the detection sensitivity of the platform. (3) The excitation wavelength of AuNCs@HDS was at 405 nm and emission wavelength was at 585 nm, which can resist various interferences from the biological matrix. All above results demonstrated that the AuNCs@HDS/H^+/urea detection system possessed excellent performance for monitoring urease.

3. 4 Urease inhibitor assay

Acetohydroxamic acid (AHA) [41], an essential drug for the treatment of urinary tract infections, as well as a pesticide (dimethoate [42]), were employed as

representative samples to assess the inhibitor detecting capability to verify its potential value of the biosensor in urease inhibitor detection. AHA and dimethoate did not affect the fluorescence of AuNCs@HDS or H^+-induced fluorescence quenching of AuNCs@HDS (**Fig. 4A** and **Fig. 4D)**, guaranteeing the specific recognition of this platform for inhibitor sensing. The fluorescence intensity of AuNCs@HDS/H^+/urea/urease showed a decreasing tendency when urease reacted with increased concentration of AHA or dimethoate (**Fig. 4B** and **Fig. 4E)**. In the range of 1-9 μM, the inhibition efficiency (IE, %) showed linear correlation with the AHA concentration (**Fig. 4C)**, and the linear equation was IE (%) = 1.7193+ 7.3062 [AHA] (μM), R^2 = 0.986, and a LOD of 0.11 μM. As for dimethoate, the inhibition efficiency gradually increased with an increase in dimethoate concentration (0.5-30 mg/L), and the linear equation was IE (%) = 0.9869 + 2.1620 [dimethoate] (mg/L), R^2 = 0.989, and a LOD of 0.41 mg/L (**Fig. 4F)**. Besides, the IC_{50} (the inhibitor concentration to inhibit 50% of the urease activity) of AHA was calculated as 6.61 μM, and IC_{50} of dimethoate was 22.67 mg/L. These results suggested that our proposed biosensor could be used to detect potential urease inhibitors.

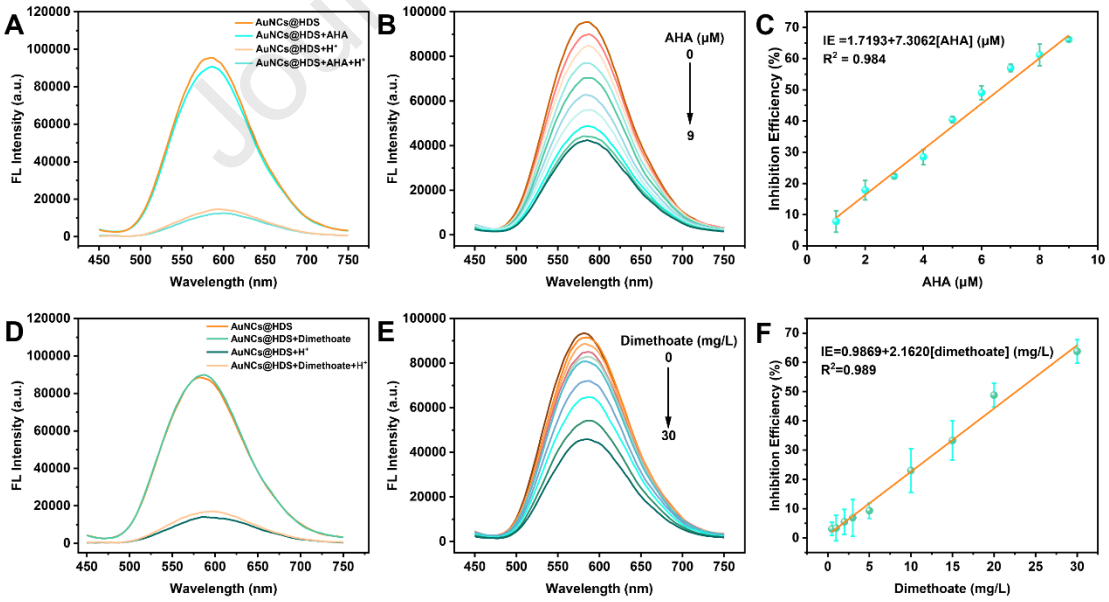

Fig. 4. Effect of AHA (A) and dimethoate (D) on the AuNCs@HDS and AuNCs@HDS/H^+/ system. FL spectra of AuNCs@HDS/H^+/urea/urease with varied AHA (B) and dimethoate concentrations (E). (C, F) The relationship between inhibition efficiency (IE) and inhibitor concentration (AHA,

dimethoate)

3. 5 Urease portable kit assay

Owing to the excellent analytical performance of the AuNCs@HDS sensing platform for urease activity, a portable kit was built for on-site analysis of urease, increasing the portability in practical use. Therefore, an AuNCs@HDS-based fluorescent hydrogel kit combined with a smartphone was prepared for the visual and quantitative on-site monitoring of urease (**Fig. 5A)**. First, the stability of the hydrogel kit was explored. There were no significant changes in the fluorescence color of the hydrogel kit after 60 min of irradiation under a UV lamp and one month of storage (**Fig. S8** and **Fig. S9)**, which indicated that the AuNCs@HDS-based hydrogel kit was stable. **Fig. 5B** inset shows an apparent change in color from pink to orange was observed with increasing urease concentration. Next, using the Color-Collection software on a smartphone, the fluorescent images were broken down into color intensity values for the red (R), green (G), and blue (B) channels, and the urease activity was quantified using the color intensity RGB values. There was a clear linear correlation between (R+G)/B and urease concentration in the range of 6.0 – 22.5 U/L, with a linear equation of (R+G)/B = 2.0121 + 0.0946 [urease] (U/L) and R^2 = 0.992 (**Fig. 5B)**. The findings indicated that the portable kit in conjunction with a smartphone provided a simple, intuitive, and easily transportable on-site quantitative assay for urease.

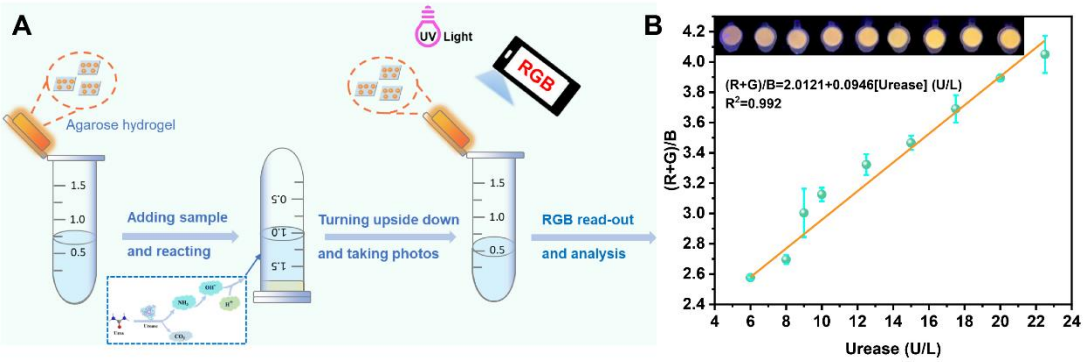

Fig. 5. (A) Schematic diagram of the procedure for the detection of urease activity using the portable agarose hydrogel kit. (B) Linearity between channel intensity ratio and the urease amount. The inset

displays UV light images of agarose hydrogel at different urease concentrations.

3. 6 Analysis of human saliva samples for urease

The detection of oral urease activity is an effective method for preventing dental caries and screening for helicobacter pylori infection [43]. To further assess the usefulness of our strategy in actual samples, the standard addition method was used to detect urease in saliva samples. **Fig. S10** shows that the human saliva samples 1 – 3 displayed no influence on the AuNCs@HDS or AuNCs@HDS/H^+, eliminating the interference from human saliva samples. As shown in Table S2 and Table S3, no urease was found in the human saliva samples provided by healthy volunteers, which was consistent with previous work [44, 45]. The recovery of urease detection by this method varied from 91.1% to 106.8%, and the relative standard deviations (RSDs) were < 6.3% (**Table S2)**. The recovery of urease detection by the portable agarose hydrogel kit varied from 95.2% to 106.6%, and the relative standard deviations (RSDs) were < 4.26% (**Table S3)**. In addition, we also used a colorimetry based on Nessler reagent to verify the accuracy of our method in detecting urease (demonstrated in **Fig. S11**). The results obtained by colorimetric method were consistent with our fluorescence method and hydrogel kit (**Table S2** and **Table S3**). These results further indicated that this constructed fluorescence sensing platform and hydrogel kit had high accuracy and reliability for detecting urease in real samples. Besides, it should also be noted that this method is limited in the medium with strong buffering ability.

4. Conclusion

Here, a simple and sensitive fluorescence sensing platform was prepared to detect urease and its inhibitors. The fluorescence sensing platform leverages the unique fluorescence enhancement effect of AuNCs induced by HDS and the specificity of urease-catalyzed hydrolysis of urea. The H^+-induced fluorescence quenching of AuNCs@HDS was combined with the OH^- production from urea-catalyzed hydrolysis of urea to achieve the changes in fluorescence response of AuNCs@HDS as an output

signal, achieving highly sensitive and precise identification of urease and urease inhibitors. According to the results of the sensitive detection of urease by the sensing platform, it was also used to detect urease in human saliva samples. The results confirmed the utility and accuracy of the sensing platform in detecting urease in the real samples. Also, an AuNCs@HDS-based hydrogel kit was prepared for the portable detection of urease combined with a smartphone. We believe that this work not only provide powerful technical support for urease-related biochemical studies and portable detection, but also give inspirations for constructing AuNCs@HDS-based sensors.

Acknowledgments

This work is supported by Shandong Provincial Natural Science Foundation, China (No. ZR2023QB126 and No. ZR2023QB145), Traditional Chinese Medical Science and Technology Foundation of Shandong Province (No. Q-2023032), the Doctoral Scientific Research Foundation of Jining Medical University (No. 601018001 and No. 601011001), and Higher Education Institutions' Youth Innovation Team of Shandong Province (No. 600768002).

Reference

[1] K. Ahmad, H.M. Asif, T. Afzal, M.A. Khan, M. Younus, U. Khurshid, M. Safdar, S. Saifulah, B. Ahmad, A. Sufyan, S.A. Ansari, H.M. Alkahtani, I.A. Ansari, Green synthesis and characterization of silver nanoparticles through the Piper cubeba ethanolic extract and their enzyme inhibitory activities, Front. Chem. 11 (2023) 1065986.

[2] L. Mazzei, F. Musiani, S. Ciurli, The structure-based reaction mechanism of urease, a nickel dependent enzyme: tale of a long debate, J. Biol. Inorg. Chem. 25 (2020) 829-845.

[3] C.R. Carlini, J.C. Polacco, Toxic properties of urease, Crop. Sci. 48 (2008) 1665-1672.

[4] R. Ligabue-Braun, F.C. Andreis, H. Verli, C.R. Carlini, 3-to-1: unraveling structural transitions in ureases, Naturwissenschaften 100 (2013) 459-67.

[5] S. Hu, Y. Gao, Y. Wu, X. Guo, Y. Ying, Y. Wen, H. Yang, Raman tracking the activity of urease in saliva for healthcare, Biosens. Bioelectron. 129 (2019) 24-28.

[6] I. Konieczna, P. Zarnowiec, M. Kwinkowski, B. Kolesinska, J. Fraczyk, Z. Kaminski, W. Kaca, Bacterial urease and its role in long-lasting human diseases, Curr. Protein Pept. Sc. 13 (2012) 789-806.

[7] J. Ni, T.C.D. Shen, E.Z. Chen, K. Bittinger, A. Bailey, M. Roggiani, A. Sirota-Madi, E.S. Friedman, L.C.A. Lin, I. Nissim, J. Scott, A. Lauder, C. Hoffmann, G. Rivas, L. Albenberg, R.N. Baldassano, J. Braun, R.J. Xavier, C.B. Clish, M. Yudkoff, H.Z. Li, M. Goulian, F.D. Bushman, J.D. Lewis, G.D. Wu, A role for bacterial urease in gut dysbiosis and Crohn's disease, Sci. Transl. Med. 9 (2017) 6888.

[8] Z.W. Jing, Y.Y. Jia, N. Wan, M. Luo, M.L. Huan, T.B. Kang, S.Y. Zhou, B.L. Zhang, Design and evaluation of novel pH-sensitive ureido-conjugated chitosan/TPP nanoparticles targeted to Helicobacter pylori, Biomaterials 84 (2016) 276-285.

[9] N. Naheed, S. Maher, F. Saleem, A. Khan, A. Wadood, S. Rasheed, M.I. Choudhary, M. Froeyen, I. Abdullah, M.U. Mirza, J.F. Trant, S. Ahmad, New isolate from salvinia molesta with antioxidant and urease inhibitory activity, Drug. Develop. Res. 82 (2021) 1169-1181.

[10] P. Kafarski, M. Talma, Recent advances in design of new urease inhibitors: a review, J. Adv. Res. 13 (2018) 101-112.

[11] L.S.B. Upadhyay, Urease inhibitors: a review, Indian J. Biotechnol. 11 (2012) 381-388.

[12] J. An, M.Z. Chen, G.Y. Liu, Y.Q. Hu, R.B. Chen, Y. Lyu, S. Sharma, Y.F. Liu, Water-stable perovskite-on-polymer fluorescent microspheres for simultaneous monitoring of pH, urea, and urease, Anal. Bioanal. Chem. 413 (2021) 1739-1747.

[13] M. Wang, S. Wang, X. Song, Z. Liang, X. Su, Photo-responsive oxidase mimic of

conjugated microporous polymer for constructing a pH-sensitive fluorescent sensor for bio-enzyme sensing, Sensor. Actuator. B Chem. 316 (2020) 128157.

[14] H. Huang, J. Li, M. Liu, Z. Wang, B. Wang, M. Li, Y. Li, pH-controlled fluorescence changes in a novel semiconducting polymer dot/pyrogallic acid system and a multifunctional sensing strategy for urea, urease, and pesticides, Anal. Methods-UK 9 (2017) 6669-6674.

[15] D.D. Hu, D. Wu, Y.M. Lu, J.Y. Liu, Z.Y. Guo, S. Wang, C.Y. Zhai, Z.H. Qing, Y.F. Hu, Protonation-induced DNA conformational-change dominated electrochemical platform for glucose oxidase and urease analysis, Anal. Chim. Acta. 1226 (2022) 340164.

[16] H.H. Deng, G.L. Hong, F.L. Lin, A.L. Liu, X.H. Xia, W. Chen, Colorimetric detection of urea, urease, and urease inhibitor based on the peroxidase-like activity of gold nanoparticles, Anal. Chim. Acta. 915 (2016) 74-80.

[17] S.H. Li, L.Y. Xiao, L.Q. Xiao, H.L. Tan, Coordination polymer nanoprobe integrated carbon dot and phenol red for turn-on fluorescence detection of urease activity, Microchim. Acta 190 (2023) 79.

[18] F.P. Shi, D.Y. Shang, Z.H. Wang, An rGQD/chitosan nanocomposite-based pH-sensitive probe: application to sensing in urease activity assays, New J. Chem. 43 (2019) 13398-13407.

[19] J.Y. Liu, J.B. Zhang, Y. Zhang, Y. Wang, M.K. Wang, Z.W. Li, G.N. Wang, X.G. Su, A pH-responsive fluorometric and colorimetric system based on silicon quantum dots and 4-nitrophenol for urease activity detection, Talanta 237 (2022) 122956.

[20] H.H. Deng, G.W. Wu, Z.Q. Zou, H.P. Peng, A.L. Liu, X.H. Lin, X.H. Xia, W. Chen, pH-Sensitive gold nanoclusters: preparation and analytical applications for urea, urease, and urease inhibitor detection, Chem. Commun. 51 (2015) 7847-7850.

[21] J.J. Li, J.J. Zhu, K. Xu, Fluorescent metal nanoclusters: from synthesis to applications, Trac-Trend. Anal. Chem. 58 (2014) 90-98.

[22] D.Z. Hao, X.L. Zhang, R.X. Su, Y.F. Wang, W. Qi, Biomolecule-protected gold nanoclusters: synthesis and biomedical applications, J. Mater. Chem. B. 11 (2023)

5051-5070.

[23] S.M. van de Looij, E.R. Hebels, M. Viola, M. Hembury, S. Oliveira, T. Vermonden, Gold nanoclusters: imaging, therapy, and theranostic roles in biomedical applications, Bioconjugate Chem. 33 (2022) 4-23.

[24] Z.K. Wu, R.C. Jin, On the ligand's role in the fluorescence of gold nanoclusters, Nano Lett. 10 (2010) 2568-2573.

[25] Q.Y. Sha, R.X. Guan, H.Y. Su, L. Zhang, B.F. Liu, Z.Y. Hu, X. Liu, Carbohydrate-protein template synthesized high mannose loading gold nanoclusters: A powerful fluorescence probe for sensitive Concanavalin A detection and specific breast cancer cell imaging, Talanta 218 (2020) 121130.

[26] R.C. Jin, Quantum sized, thiolate-protected gold nanoclusters, Nanoscale 2 (2010) 343-362.

[27] F.Y. Mo, Z.Y. Ma, T.T. Wu, M.L. Liu, Y.Y. Zhang, H.T. Li, S.Z. Yao, Holey reduced graphene oxide inducing sensitivity enhanced detection nanoplatform for cadmium ions based on glutathione-gold nanocluster, Sensor. Actuator. B Chem. 281 (2019) 486-492.

[28] X.Y. Sun, R.Z. Wen, R.M. Zhang, Y.X. Guo, H.C. Li, Y.I. Lee, Engineering a ratiometric-sensing platform based on a PTA-NH_2@GSH-AuNCs composite for the visual detection of copper ions via RGB assay, Microchem. J. 182 (2022) 107877.

[29] Q. Gao, S.Y. Xu, C. Guo, Y.G. Chen, L.Y. Wang, Embedding nanocluster in MOF via crystalline ion-triggered growth strategy for improved emission and selective sensing, Acs Appl. Mater. Inter. 10 (2018) 16059-16065.

[30] Y. Cai, Z.Y. Qiu, X.B. Lin, W. Zeng, Y.R. Cao, W.P. Liu, Y.J. Liu, Self-assembled nanomaterials based on aggregation-induced emission of AuNCs: Fluorescence and colorimetric dual-mode biosensing of organophosphorus pesticides, Sensor. Actuator. B Chem. 321 (2020) 128481.

[31] J.Y. Lu, C.X. Xu, Z.S. Tian, J.F. Lu, Y. Lin, Z.L. Shi, Green emission and Ag^+ sensing of hydroxy double salt supported gold nanoclusters, Nanoscale 8 (2016) 5120-5125.

[32] J.W. Zhao, X.G. Kong, W.Y. Shi, M.F. Shao, J.B. Han, M. Wei, D.G. Evans, X.

Duan, Self-assembly of layered double hydroxide nanosheets/Au nanoparticles ultrathin films for enzyme-free electrocatalysis of glucose, J. Mater. Chem. 21 (2011) 13926-13933.

[33] G.L. Fan, F. Li, D.G. Evans, X. Duan, Catalytic applications of layered double hydroxides: recent advances and perspectives, Chem. Soc. Rev. 43 (2014) 7040-7066.

[34] G.R. Williams, J. Crowder, J.C. Burley, A.M. Fogg, The selective intercalation of organic carboxylates and sulfonates into hydroxy double salts, J. Mater. Chem. 22 (2012) 13600-13611.

[35] M. Wang, Y. Han, R. Huang, Z. Wang, G. Wang, Confinement of gold nanoclusters on hydroxy double salt for versatile fluorescent sensing of bio-enzymes, Sensor. Actuator. B Chem. 401 (2024) 135038.

[36] Z. Luo, X. Yuan, Y. Yu, Q. Zhang, D.T. Leong, J.Y. Lee, J. Xie, From aggregation-induced emission of Au(I)-thiolate complexes to ultrabright Au(0)@Au(I)-thiolate core-shell nanoclusters, J. Am. Chem. Soc. 134 (2012) 16662-70.

[37] Y.Y. Zhang, H.D. Xu, Y. Chen, X.S. You, Y.X. Pu, W.F. Xu, X.L. Liao, High-sensitivity detection of cysteine and glutathione using Au nanoclusters based on aggregation-induced emission, J. Fluoresc. 30 (2020) 1491-1498.

[38] S.D. Qi, H.S. Al-mashriqi, A. Salah, H.L. Zhai, Glutathione capped gold nanoclusters-based fluorescence probe for highly sensitive and selective detection of transferrin in serum, Microchem. J. 175 (2022) 107163.

[39] T. Biswick, D.-H. Park, Y.-G. Shul, J.-H. Choy, P-coumaric acid–zinc basic salt nanohybrid for controlled release and sustained antioxidant activity, J. Phys. Chem. Solids 71 (2010) 647-649.

[40] L. Rastogi, A.J. Kora, J. Arunachalam, Highly stable, protein capped gold nanoparticles as effective drug delivery vehicles for amino-glycosidic antibiotics, Mat. Sci. Eng. C-Mater. 32 (2012) 1571-1577.

[41] S. Milo, R.A. Heylen, J. Glancy, G.T. Williams, B.L. Patenall, H.J. Hathaway, N.T. Thet, S.L. Allinson, M. Laabei, A.T.A. Jenkins, A small-molecular inhibitor against Proteus mirabilis urease to treat catheter-associated urinary tract infections, Sci. Rep-

Uk. 11 (2021) 3726.

[42] H. Huang, J. Li, M.X. Liu, Z.Z. Wang, B.D. Wang, M.N. Li, Y.X. Li, pH-controlled fluorescence changes in a novel semiconducting polymer dot/pyrogallic acid system and a multifunctional sensing strategy for urea, urease, and pesticides, Anal. Methods-UK. 9 (2017) 6669-6674.

[43] G. Dahlen, H. Hassan, S. Blomqvist, A. Carlen, Rapid urease test (RUT) for evaluation of urease activity in oral bacteria in vitro and in supragingival dental plaque ex vivo, Bmc Oral Health 18 (2018) 89.

[44] M. Wang, S. Wang, X. Song, Z. Liang, X. Su, Photo-responsive oxidase mimic of conjugated microporous polymer for constructing a pH-sensitive fluorescent sensor for bio-enzyme sensing, Sensor. Actuator. B Chem. 316 (2020) 128157.

[45] J.Y. Liu, J.B. Zhang, Y. Zhang, Y. Wang, M.K. Wang, Z.W. Li, et al., A pH-responsive fluorometric and colorimetric system based on silicon quantum dots and 4-nitrophenol for urease activity detection, Talanta 237 (2022) 122956.

Highlights

- The AuNCs@HDS with excellent fluorescence property was strategically designed.
- The AuNCs@HDS system had good sensitivity and fast response to pH.
- A AuNCs@HDS-based sensor was constructed for urease and its drug inhibitors.
- This assay realized the urease analysis in saliva samples with robust performance.
- A portable and low-cost hydrogel kit was fabricated for urease analysis.

Declaration of interests

☒ The authors declare that they have no known competing financial interests or personal relationships that could have appeared to influence the work reported in this paper.

☐The authors declare the following financial interests/personal relationships which may be considered as potential competing interests: